Structural Engineering and Mechanics, Vol. 29, No. 5 (2008) 581-597
DOI: http://dx.doi.org/10.12989/sem.2008.29.5.581

Double displacement coupled forced response for electromechanical integrated electrostatic harmonic drive

Lizhong Xu†, Cuirong Zhu and Lei Qin

Mechanical engineering institute, Yanshan University, Qinhuangdao 066004, China

(Received November 10, 2007, Accepted March 20, 2008)

Abstract. In this paper, the double displacement coupled statics and dynamics of the electromechanical integrated electrostatic harmonic drive are developed. The linearization of the nonlinear dynamic equations is completed. Based on natural frequency and mode function, the double displacement coupled forced response of the drive system to voltage excitation are obtained. Changes of the forced response along with the system parameters are investigated. The voltage excitation can cause the radial and tangent coupled forced responses of the flexible ring. The flexible ring radius, ring thickness and clearance between the ring and stator have obvious influences on the double displacement coupled forced responses.

Keywords: electromechanical integrated; Harmonic drive; forced response; voltage excitation.

1. Introduction

Micro-electromechanical system (MEMS) can be described as machines constructed of small moving sub-elements that have characteristic dimensions in the range of about 0.5-500 μm. Such devices have potential applications in electronic assembly, medical, microspacecraft and military equipment. The MEMS devices require high integration of the mechanical, electric and control techniques (Thielicke and Obermeier 2000, Giuseppe 2007, Bao and Mukherjee 2004).

Author invents an electromechanical integrated electrostatic harmonic drive as shown in Fig. 1. The drive mainly consists of a flexible ring and an outer ring stator. The outer ring stator electrodes are applied to voltage sequentially, and a rotational electric field will be produced which will result in a periodic elastic deformation of the flexible ring and the periodic capacity changes between flexible ring and stator. It produces tangential electric field forces to drive the axis to rotate. As the stator is fixed, electric potential is applied to each segment of the outer ring with small screw. The flexible ring is supported on output axis which is put to earth. Thus, the flexible ring is put to earth. Hence, the voltage between the inner ring and a segment of the outer ring can be produced without brushes or sliding contacts. In the drive, integration of the harmonic drive, motor and control can be realized. It is a new concept of the electromechanical drive system (Xu *et al.* 2007). Compared with piezoelectric and electromagnetic actuation principles (Oliver 2000, Wu *et al.* 2006, Lizhong and Xiuhong 2007), the electromechanical integrated electrostatic harmonic drive needs neither

† Ph.D., Corresponding author, E-mail: Xlz@ysu.edu.cn

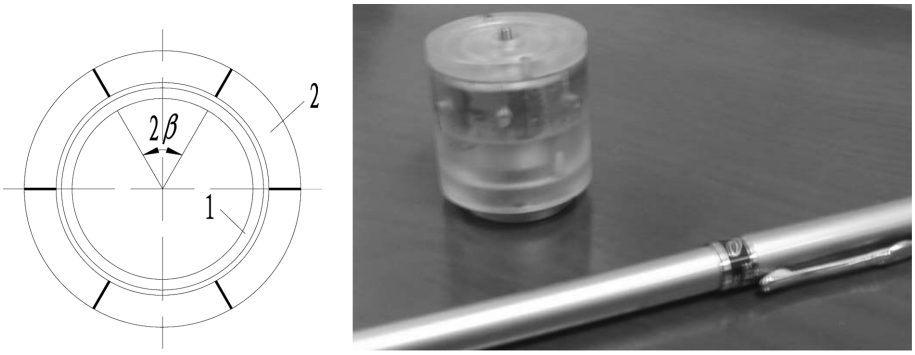

(a) (b)

Fig. 1 An electromechanical integrated harmonic drive (1-Flexible ring, 2-Outer ring stator)

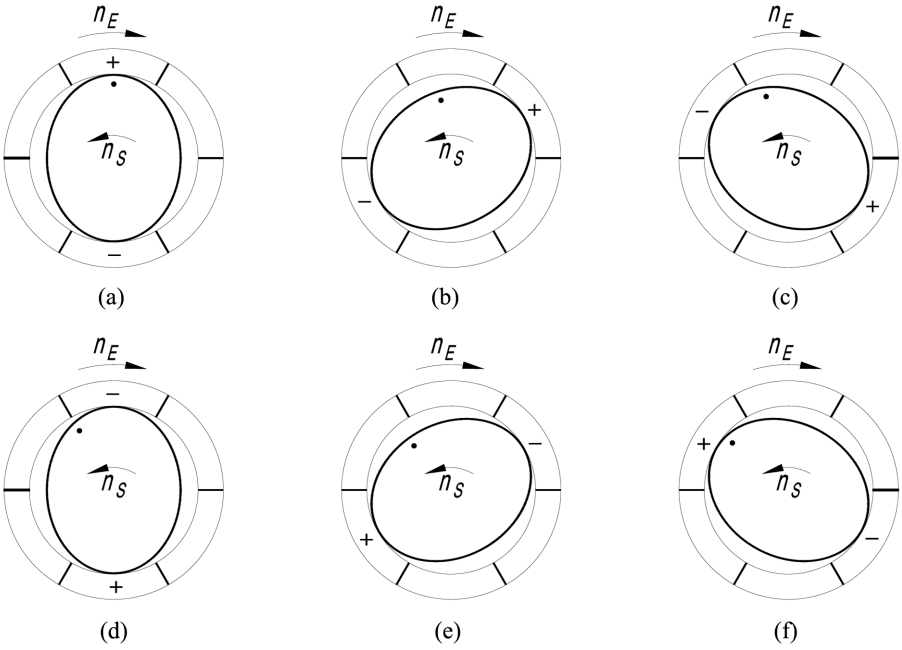

(a) (b) (c)

(d) (e) (f)

Fig. 2 The operation of electromechanical integrated electrostatic harmonic drive

additional elements like coils or cores, nor special materials like piezoelectric ceramics. It is more favorable for miniaturization of the electromechanical devices. Compared with other electrostatic actuation principles (Sarros *et al.* 2002, Nadal-Guardia *et al.* 2003, Bao and Mukherjee 2004), the drive does not require fabrication of the teeth on microelements and its rotational axis does not wobble. Thus the device reported here is easier to fabricate and use. The drive also offers other advantages such as higher load-carrying capacity and low required precision of fabrication.

Fig. 2 shows the operation for a six-segment rotary electric field electromechanical integrated harmonic actuator. Initially, a voltage is applied between the flexible ring and segments 1 (positive potential) and 4 (negative potential) causing an elastic deformation of the flexible ring as shown in Fig. 2(a). Next, a voltage is applied between the flexible ring and segments 2 (positive potential)

and 5 (negative potential) causing an elastic deformation of the flexible ring as shown in Fig. 2(b). Voltages are then applied sequentially to segments 3 (positive potential) and 6 (negative potential) as shown in Fig. 2(c), 4 (positive potential) and 1 (negative potential) as shown in Fig. 2(d), 5 (positive potential) and 2 (negative potential) as shown in Fig. 2(e), and 6 (positive potential) and 3 (negative potential) as shown in Fig. 2(f), which completes one electrical cycle. Note that the position of the black dot shown in Fig. 5(f) has rotated slightly after one complete electrical cycle compared to its initial position in Fig. 2(a). Note that the flexible ring rotates in the opposite direction to the electrical excitation sequence as shown as arrow in Fig. 2.

The dynamics of the microsystems is an important subject that should be developed. Understanding the dynamic behavior of MEMS is very important for controlling their performance.

In this paper, the double displacement coupled statics and dynamics of the electromechanical integrated electrostatic harmonic drive are developed. The linearization of the nonlinear dynamic equations is completed. Based on analysis of natural frequency and vibrating modes, the double displacement coupled forced responses of the drive system to voltage excitation are obtained. Changes of the forced response along with the system parameters are investigated as well. Results show: the voltage excitation can cause the radial and tangent forced responses of the micro flexible ring; for given simple harmonic voltage excitation, the forced responses are also simple harmonic vibration; the flexible ring radius, ring thickness and clearance between the ring and stator have obvious influences on the double displacement coupled forced responses; in order to get good dynamic performance, smaller clearance, thickness and radius should be selected. These results can be used to design and manufacture of the drive system and can offer some reference for other micro electromechanical systems.

2. Electromechanical coupled statics

The dynamic equation of micro flexible ring subjected to force is

$$\left.\begin{aligned} \frac{1}{r}\frac{\partial^2}{\partial\theta^2}\left[\frac{EI_x}{r^2}\left(\frac{\partial v}{\partial\theta}-\frac{\partial^2 u}{\partial\theta^2}\right)\right]-EA\left(\frac{u}{r}+\frac{1}{r}\frac{\partial v}{\partial\theta}\right) &= -q_r r+\rho A\ddot{u}r \\ EA\frac{\partial}{\partial\theta}\left(\frac{u}{r}+\frac{1}{r}\frac{\partial v}{\partial\theta}\right)+\frac{1}{r}\frac{\partial}{\partial\theta}\left[\frac{EI_x}{r^2}\left(\frac{\partial v}{\partial\theta}-\frac{\partial^2 u}{\partial\theta^2}\right)\right] &= -q_t r+\rho A\ddot{v}r \end{aligned}\right\} \tag{1}$$

where u and v are radial and tangential displacements of the micro ring, respectively; $\ddot{u}$ and $\ddot{v}$ are the second derivatives of displacement u and v with respect to time, respectively; r is the average radius of the ring. A is its transverse section area; ρ is material density of the ring; E is the modulus of elasticity of the ring material; I_x is section modular of the ring, $I_x = ld^3/12$ (l and d is effective width and the thickness of micro ring, respectively); θ is position angle of the micro ring; q_r and q_t are radial and tangential loads per unit arc length applied to the flexible ring, respectively.

From Eq. (1), let $\ddot{u} = 0$, $\ddot{v} = 0$, and $v = \partial u/\partial\theta$, balance equation of the ring is obtained as below

$$u+2\frac{\partial^2 u}{\partial\theta^2}+\frac{\partial^4 u}{\partial\theta^4}=\frac{r^2}{EA}\left(q_r-\frac{\partial q_t}{\partial\theta}\right) \tag{2}$$

A micro flexible ring under electrical field force is shown in Fig. 3. The micro ring is inside an

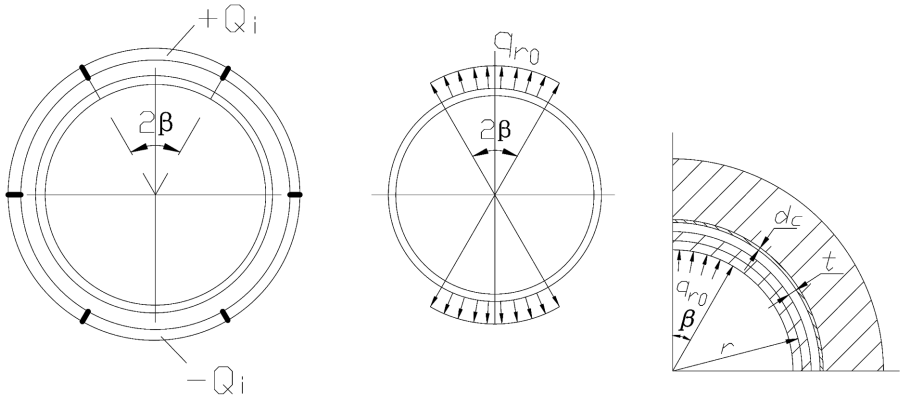

Fig. 3 A micro flexible ring subjected to electrical field force

outer ring stator which consists of a number of conductive segments with an insulating layer between the micro ring and outer ring and also between adjacent segments. The central angle of each segment is 2β. When a voltage is applied between a segment of the outer ring and the micro ring, a distributed electrical field force is subjected to the micro ring. Using Rayleigh-Ritz method, the displacement distribution is investigated (Xu and Qin 2007). The results show that the maximum error is about 7% when assumption that the electric field force is uniform is used. For simplifying analysis, the uiniform electric field force assumption is used here. Assuming that the electrical field force is uniformly distributed on the micro ring, the radial and tangential electric field forces per unit arc length can be denoted by symbol q_{r0} and q_{t0} which are applied to micro ring, through the central angle $[-\beta, \beta]$.

Let w denote the radial relative distance between the flexible ring and outer stator, and the radial electrical field force F_e between them can be given

$$F_e = -\frac{1}{2} v_{is}^2 \frac{dC}{dw} \tag{3}$$

Where v_{is} and C are voltage and capacitance between the flexible ring and outer stator, respectively.

The clearance between the micro flexible ring and the outer stator is so small that the capacity between them can be calculated by equation of flat capacitor

$$C = \frac{\beta}{\pi} \cdot \frac{\varepsilon_0 \cdot 2\pi r l}{t - \bar{u}_0 + d_c/\varepsilon_r} \tag{4}$$

Where ε_0 is permittivity constant of free space, $\varepsilon_0 = 8.85 \times 10^{-12}\ C^2 \cdot N^{-1} \cdot m^{-2}$, ε_r is relative dielectric constant of the insulating layer, t is initial clearance between micro ring and outer ring, d_c is width of the insulating layer, $\bar{u}_0$ is average radial displacement of the micro ring within central angle $[-\beta, \beta]$.

Combining Eq. (3) with Eq. (4), the radial electric force q_{r0} between the micro ring and a segment of the outer stator ring per unit arc length can be calculated as following

$$q_{r0} = \frac{F_e}{2\beta r} = \frac{v_{is}^2 \varepsilon_0 l}{2(t - \bar{u}_0 + d_c/\varepsilon_r)^2} \tag{5}$$

Here neglecting tangential load, and then the static load distribution on the micro ring is shown as below

When $-\beta \le \theta \le \beta$ and $\pi - \beta \le \theta \le \pi + \beta$, $q_{rs} = \dfrac{v_{is0}^2 \varepsilon_0 l}{2(t - \bar{u}_0 + d_c/\varepsilon_r)^2}$

When $\beta \le \theta \le \pi - \beta$ and $\pi + \beta \le \theta \le 2\pi - \beta$, $q_{rs} = 0$

The load can be defined in Fourier series form as

$$q_{rs} = q_0 + \sum_1^{\infty} q_k \cos k\theta \tag{6}$$

Where $q_0 = \dfrac{2q_r\beta}{\pi}$, $q_k = \dfrac{4q_{r0}}{\pi k}\sin k\beta$

Let static displacement $u = \sum_{k=2,4,6,\ldots} C_k \cos k\theta$, and substituting it and Eq. (6) into Eq. (2), yields

$$u = \frac{4q_{r0}r^2}{\pi EA} \sum_{k=2,4,6,\ldots} \frac{\sin k\beta}{k(k^2-1)^2} \cos k\theta \tag{7}$$

The average radial displacement $\bar{u}_0$ of the flexible ring can be calculated as below

$$\bar{u}_0 = \frac{1}{2\beta}\int_{-\beta}^{\beta} u d\theta = \frac{4q_{r0}r^2}{\pi EA\beta} \sum_{k=2,4,6,\ldots} \frac{\sin^2 k\beta}{k^2(k^2-1)^2} \tag{8}$$

3. Electromechanical coupled dynamics

In Eq. (1), compared with radius r of the ring, the transverse section size of the micro flexible ring is so small that term I_x is much smaller than term Ar^2. So the term EI_x in Eq. (1) can be neglected and Eq. (1) is simplified as

$$\left.\begin{aligned} u + \frac{\partial v}{\partial \theta} + \rho\frac{r^2}{E}\ddot{u} - \frac{q_r r^2}{AE} &= 0 \\ \frac{\partial}{\partial\theta}\left(u + \frac{\partial v}{\partial\theta}\right) - \rho\frac{r^2}{E}\ddot{v} + \frac{q_t r^2}{AE} &= 0 \end{aligned}\right\} \tag{9}$$

The total radial displacement u of the micro flexible ring consists of the static displacement u_0 and the dynamic displacement Δu

$$u = u_0 + \Delta u \tag{10}$$

The total tangential displacement v consists of the static displacement v_0 and the dynamic displacement Δv

$$v = v_0 + \Delta v \tag{11}$$

The change of the displacement results in changes of the capacity, voltage and electric field force

between micro flexible ring and outer stator. Then, the total capacity C consists of the static capacity C_0 and the dynamic capacity ΔC

$$C = C_0 + \Delta C = C_0 + \left.\frac{dC}{dw}\right|_{w_0} \Delta w \tag{12}$$

Where distance $w = t - u$, Δw is dynamic component of the distance corresponding to dynamic displacement Δu, w_0 is static component of the distance corresponding to static displacement u_0.

Total voltage v_{is} consists of the static voltage v_{is0} and the dynamic one Δv_{is}

$$v_{is} = v_{is0} + \Delta v_{is} \tag{13}$$

The total radial electric field force F_e consists of the static electric field force F_0 and the dynamic one ΔF_e

$$F_e = F_0 + \Delta F_e \tag{14}$$

Then, the radial load q_r per unit arc length on the micro ring consists of the static component q_{rs} and the dynamic one Δq_r

$$q_r = q_{rs} + \Delta q_r \tag{15}$$

The tangential load q_t per unit arc length on the micro ring consists of the static component q_{ts} and the dynamic one Δq_t

$$q_t = q_{ts} + \Delta q_t \tag{16}$$

Substituting Eqs. (12), (13) and (14) into Eq. (3), neglecting the higher order term, yields

$$F_0 = -\frac{1}{2} v_{is0}^2 \left.\frac{dC}{dw}\right|_{w_0} \tag{17}$$

$$\Delta F_e = -\frac{1}{2}\left\{ v_{is0}^2 \left.\frac{d^2C}{dw^2}\right|_{w_0} \Delta w + 2 v_{is0} \left.\frac{dC}{dw}\right|_{w_0} \Delta v_{is} \right\} \tag{18}$$

When the voltage is stable, it is reasonable assuming that $\Delta v_{is} \approx 0$. Substituting Eqs. (17) and (18) into Eq. (5), yields the following equation

$$q_{rs} = \frac{v_{is0}^2 \varepsilon_0 l}{2(t - \bar{u}_0 + d_c/\varepsilon_r)^2} \tag{19}$$

$$\Delta q_r = \Delta F_e / 2\beta r = -\frac{1}{2} v_{is0}^2 \left.\frac{d^2 C_i}{dw^2}\right|_{w_0} \Delta w / 2\beta r = -\frac{v_0^2 \varepsilon_0 l}{(t - \bar{u}_0 + d_c/\varepsilon_r)^3} \Delta w \tag{20}$$

Substituting Eqs. (10), (11), (19) and (20) into Eq. (9), neglecting the higher order term, yields the following equation

$$\left.\begin{aligned} \Delta u + \frac{\partial \Delta v}{\partial \theta} + \rho \frac{r^2}{E} \Delta \ddot{u} - \frac{\Delta q_r r^2}{AE} = 0 \\ \frac{\partial}{\partial \theta}\left(\Delta u + \frac{\partial \Delta v}{\partial \theta}\right) - \rho \frac{r^2}{E} \Delta \ddot{v} + \frac{\Delta q_t r^2}{AE} = 0 \end{aligned}\right\} \tag{21}$$

Eq. (21) is linear electromechanical coupled dynamic equation of the micro ring subjected to electric field force.

Because of the structure and load symmetry of the micro ring, the dynamic displacements of the ring can be calculated on one-quarter of the micro ring. The dynamic load Δq_r is distributed as below

$$\Delta q_r = \frac{v_{is0}^2 \varepsilon_0 l}{(t - \bar{u}_0 + d_c/\varepsilon_r)^3} \Delta u \qquad (0 \le \theta \le \beta) \tag{22}$$

$$\Delta q_r = 0 \qquad \left(\beta \le \theta \le \frac{\pi}{2}\right) \tag{23}$$

Neglecting tangential load, substituting Eqs. (22) and (23) into Eq. (21), yields

$$\left.\begin{aligned} \Delta u_1 + \frac{\partial \Delta v_1}{\partial \theta} + \rho \frac{r^2}{E} \Delta \ddot{u}_1 - \frac{r^2}{AE} \frac{v_0^2 \varepsilon_0 l}{(t - \bar{u}_0 + d_c/\varepsilon_r)^3} \Delta u_1 = 0 \\ \frac{\partial}{\partial \theta}\left(\Delta u_1 + \frac{\partial \Delta v_1}{\partial \theta}\right) - \rho \frac{r^2}{E} \Delta \ddot{v}_1 = 0 \end{aligned}\right\} \qquad (0 \le \theta \le \beta) \tag{24}$$

$$\left.\begin{aligned} \Delta u_2 + \frac{\partial \Delta v_2}{\partial \theta} + \rho \frac{r^2}{E} \Delta \ddot{u}_2 = 0 \\ \frac{\partial}{\partial \theta}\left(\Delta u_2 + \frac{\partial \Delta v_2}{\partial \theta}\right) - \rho \frac{r^2}{E} \Delta \ddot{v}_2 = 0 \end{aligned}\right\} \qquad \left(\beta \le \theta \le \frac{\pi}{2}\right) \tag{25}$$

Let $\Delta u = \phi_u(\theta) q(t)$ and $\Delta v = \phi_v(\theta) q(t)$, substituting them into Eqs. (24) and (25), yields

$$\left.\begin{aligned} \phi_{u1} = -\frac{m_1}{K_{11}} A_1 \cos m_1 \theta + \frac{m_1}{K_{11}} A_2 \sin m_1 \theta \\ \phi_{v1} = A_1 \sin m_1 \theta + A_2 \cos m_1 \theta \end{aligned}\right\} \tag{26}$$

$$\left.\begin{aligned} \phi_{u2} = -\frac{m_2}{K_{12}} A_3 \cos m_2 \theta + \frac{m_2}{K_{12}} A_4 \sin m_2 \theta \\ \phi_{v2} = A_3 \sin m_2 \theta + A_4 \cos m_2 \theta \end{aligned}\right\} \tag{27}$$

Where $K_{11} = P - K_2$, $K_{12} = 1 - K_2$, $m_1 = \sqrt{\frac{K_{11} K_2}{K_{11} - 1}}$, $m_2 = \sqrt{\frac{K_{12} K_2}{K_{12} - 1}}$, $K_2 = K\omega_i^2$, $K = \rho \frac{r^2}{E}$, $P = 1 - \frac{r^2 v_{is0}^2 \varepsilon_0 l}{AE(t_0 - \bar{u}_0 + d_c/\varepsilon_r)^3}$, ω_i is ith natural frequency of the system.

Constants $A_j (j = 1, 2, 3, 4)$ are obtained by conditions of micro ring symmetry and continuity between different sections. The natural frequencies and modes function of the ring vibrations can be obtained simultaneously as well.

4. Forced response to voltage excitation

From Eq. (18), it is known that under variable voltage, dynamic electrical field force will be caused

$$\Delta F_e = -v_{is0} \left. \frac{dC_i}{dw} \right|_{w_0} \Delta v_{is} \tag{28}$$

The forced response of the system to voltage excitation will occur. The voltage is applied between the flexible ring and one of the stator segments through central angle range $[-\beta, \beta]$. Hence, under periodic exciting voltage $\Delta v_{is} = v_a \sin \omega_z t$ (Here, ω_z is the exciting frequency of the voltage), the exciting electrical field force ΔF_e can be given as below

$$\Delta F_e = -v_{is0} \left. \frac{dC_i}{dw} \right|_{w_0} v_a \sin \omega_z t \tag{29}$$

Then, within angle range $[-\beta, \beta]$, exciting electrical field force f_0 per unit arc length is

$$f_0 = \frac{\Delta F_e}{2\beta r} = \frac{v_{is0} \varepsilon_0 l}{(t_0 - \bar{u}_0 + d_c / \varepsilon_r)^2} v_a \sin \omega_z t \tag{30}$$

Therefore, the exciting force distribution on the ring is as below
When $-\beta \le \theta \le \beta$ and $\pi - \beta \le \theta \le \pi + \beta$, $\Delta q_r = f_0$
When $\beta \le \theta \le \pi - \beta$ and $\pi + \beta \le \theta \le 2\pi - \beta$, $\Delta q_r = 0$
The exciting force can also be defined in Fourier series form as

$$\Delta q_r = \frac{2 f_0}{\pi} \left(\beta + 2 \sum_{k = 2, 4, 6, \ldots} \frac{\sin k\beta}{k} \cos k\theta \right) \tag{31}$$

Let $Q_i(t)$ and $q_i(t)$ denote generalized force and generalized coordinate, then

$$Q_i(t) = \int_0^{\beta} \Delta q_r \phi_{1i}(\theta) d\theta + \int_{\beta}^{\pi/2} \Delta q_r \phi_{2i}(\theta) d\theta \qquad i = (1, 2, \ldots) \tag{32}$$

$$q_i(t) = \frac{1}{\omega_i} \int_0^t Q_i(\tau) \sin \omega_i (t - \tau) d\tau + q_i(0) \cos \omega_i t + \frac{\dot{q}_i(0)}{\omega_i} \sin \omega_i t \qquad i = (1, 2, \ldots) \tag{33}$$

Where initial values $q_i(0)$ and $\dot{q}_i(0)$ of the generalized coordinate can be determined by initial condition (here they are taken as zero). Then, above equation is simplified as

$$q_i(t) = \frac{1}{\omega_i} \int_0^t Q_i(\tau) \sin \omega_i (t - \tau) d\tau \tag{34}$$

The dynamic vibrating displacements of the system are

$$\Delta u(\theta,t) = \sum_{i=1}^{\infty} \phi_{ui}(\theta) q_i(t) \tag{35}$$

$$\Delta v(\theta,t) = \sum_{i=1}^{\infty} \phi_{vi}(\theta) q_i(t) \tag{36}$$

Substituting radial vibration mode function into Eq. (32), the generalized force $Q_{ui}(t)$ corresponding to mode i $(i = 1, 2, 3, \ldots, \infty)$ can be given

$$Q_{ui}(t) = \int_0^{\beta} \Delta q_r \left[-\frac{m_1}{K_{11}} A_1 \cos m_1\theta + \frac{m_1}{K_{11}} A_2 \sin m_1\theta \right] d\theta + \int_{\beta}^{\pi/2} \Delta q_r \left[-\frac{m_2}{K_{12}} A_3 \cos m_2\theta + \frac{m_2}{K_{12}} A_4 \sin m_2\theta \right] d\theta$$
$$= (L_{ui1} + L_{ui2}) f_0 \tag{37}$$

Where

$$L_{ui1} = -\frac{2\beta}{\pi K_{11}} \{ A_1 \sin(m_1\beta) + A_2 [\cos(m_1\beta) - 1] \} - \frac{4m_1}{\pi K_{11}} \sum_{k=2,4,6,\ldots} \frac{\sin(k\beta)}{k} \cdot$$
$$\left\{ \frac{A_1 \sin(k+m_1)\beta}{2(k+m_1)} + \frac{A_1 \sin(k-m_1)\beta}{2(k-m_1)} + \frac{A_2[\cos(k+m_1)\beta - 1]}{2(k+m_1)} - \frac{A_2[\cos(k-m_1)\beta - 1]}{2(k-m_1)} \right\}$$

$$L_{ui2} = -\frac{2\beta}{\pi K_{12}} \left\{ A_3 \left[\sin\left(\frac{\pi}{2} m_2\right) - \sin(m_2\beta) \right] + A_4 \left[\cos\left(\frac{\pi}{2} m_2\right) - \cos(m_2\beta) \right] \right\}$$

$$- \frac{4m_2}{\pi K_{12}} \sum_{k=2,4,6,\ldots} \frac{\sin(k\beta)}{k} \left\{ A_3 \cdot \frac{\sin\left[(k+m_2)\frac{\pi}{2}\right] - \sin[(k+m_2)\beta]}{2(k+m_2)} + A_3 \cdot \frac{\sin\left[(k-m_2)\frac{\pi}{2}\right] - \sin[(k-m_2)\beta]}{2(k-m_2)} \right.$$
$$\left. + A_4 \cdot \frac{\cos\left[(k+m_2)\frac{\pi}{2}\right] - \cos[(k+m_2)\beta]}{2(k+m_2)} - A_4 \cdot \frac{\cos\left[(k-m_2)\frac{\pi}{2}\right] - \cos[(k-m_2)\beta]}{2(k-m_2)} \right\}$$

Substituting tangent vibration mode function into Eq. (32), the generalized force $Q_{vi}(t)$ corresponding to mode i $(i = 1, 2, 3, \ldots, \infty)$ can be given

$$Q_{vi}(t) = \int_0^{\beta} \Delta q_r [A_1 \sin m_1\theta + A_2 \cos m_1\theta] d\theta + \int_{\beta}^{\pi/2} \Delta q_r [A_3 \sin m_2\theta + A_4 \cos m_2\theta] d\theta = (L_{vi1} + L_{vi2}) f_0 \tag{38}$$

Where

$$L_{vi1} = \frac{2\beta}{\pi m_1} \{ -A_1 [\cos(m_1\beta) - 1] + A_2 \sin(m_1\beta) \} + \frac{4}{\pi} \sum_{k=2,4,6,\ldots} \frac{\sin(k\beta)}{k} \cdot$$
$$\left\{ -\frac{A_1[\cos(k+m_1)\beta - 1]}{2(k+m_1)} + \frac{A_1[\cos(k-m_1)\beta - 1]}{2(k-m_1)} + \frac{A_2 \sin(k+m_1)\beta}{2(k+m_1)} + \frac{A_2 \sin(k-m_1)\beta}{2(k-m_1)} \right\}$$

$$L_{vi2} = \frac{2\beta}{\pi m_2}\left\{-A_3\left[\cos\left(m_2\frac{\pi}{2}\right)-\cos(m_2\beta)\right]+A_4\left[\sin\left(m_2\frac{\pi}{2}\right)-\sin(m_2\beta)\right]\right\}$$

$$+\frac{4}{\pi}\sum_{k=2,4,6,\ldots}\frac{\sin(k\beta)}{k}\cdot\left\{\frac{A_2\left[\sin(k-m_1)\frac{\pi}{2}-\sin(k-m_1)\beta\right]}{2(k-m_1)}-\frac{A_3\left[\cos(k+m_2)\frac{\pi}{2}-\cos(k+m_2)\beta\right]}{2(k+m_2)}\right.$$

$$\left.+\frac{A_3\left[\cos(k-m_2)\frac{\pi}{2}-\cos(k-m_2)\beta\right]}{2(k-m_2)}+\frac{A_4\left[\sin(k+m_1)\frac{\pi}{2}-\sin(k+m_1)\beta\right]}{2(k+m_1)}\right\}$$

Substituting generalized forces into Eq. (34), the generalized coordinates can be given

$$q_i(t) = \frac{1}{\omega_i}(L_{i1}+L_{i2})\frac{v_{is0}\varepsilon_0 l v_a}{(t_0-\bar{u}_0+d_c/\varepsilon_r)^2}\cdot\frac{1}{\omega_z^2-\omega_i^2}(\omega_i\sin\omega_z t-\omega_z\sin\omega_i t) \tag{39}$$

Where $L_{i1} = L_{iu1}+L_{iv1}$, $L_{i2} = L_{iu2}+L_{iv2}$.

In Eq. (39), the forced responses and associated free vibration are included. The associated free vibration will vanish soon under action of the damp. Therefore, this term can be not considered. Then, Eq. (39) is simplified as

$$q_i(t) = \frac{1}{\omega_i}(L_{i1}+L_{i2})\frac{v_{is0}\varepsilon_0 l v_a}{(t_0-\bar{u}_0+d_c/\varepsilon_r)^2}\cdot\frac{1}{\omega_z^2-\omega_i^2}\omega_i\sin\omega_z t \tag{40}$$

Combining Eqs. (26), (27), (40) with Eqs. (35) and (36), the forced response of the electromechanical integrated electrostatic harmonic drive system to exciting voltage can be given.

5. Results and discussions

5.1 Results and analysis

Above equations are utilized for the analysis of the forced responses of the electromechanical integrated electrostatic harmonic drive system to exciting voltage. The parameters of the numerical example are shown in Table 1. By Eqs. (26) and (27), the natural frequencies of the drive system are obtained as shown in Table 2. The forced responses corresponding to each mode and the total

Table 1 Parameters of the electromechanical coupled dynamic system with micro ring

r (mm)	t (μm)	d (μm)	l (mm)	d_c (μm)	ε_r	E (Gpa)	β (^{0})
1	2	30	1	0.5	8.4	70	30

Table 2 The first four natural frequencies of micro ring (rad/s)

Order	1	2	3	4
Natural frequency	11221155	20691843	30526243	40460281

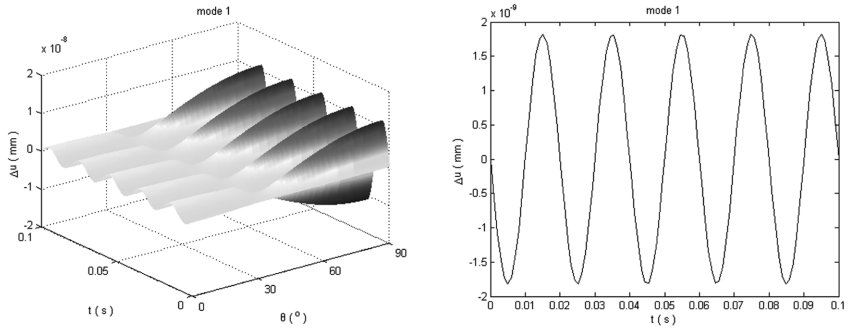

(a) Radial forced response displacement(mode one)

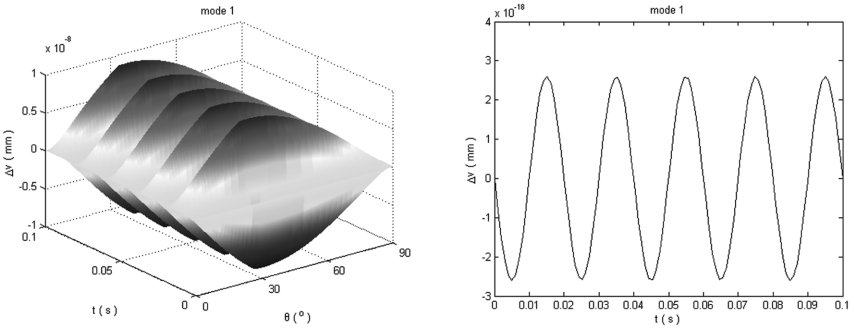

(b) Tangent forced response displacement(mode one)

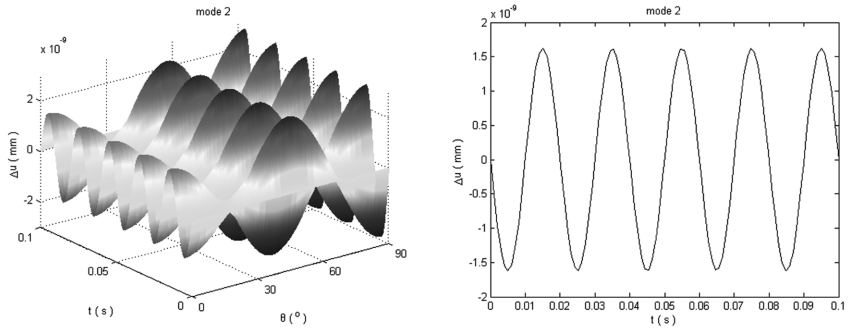

(c) Radial forced response displacement (mode two)

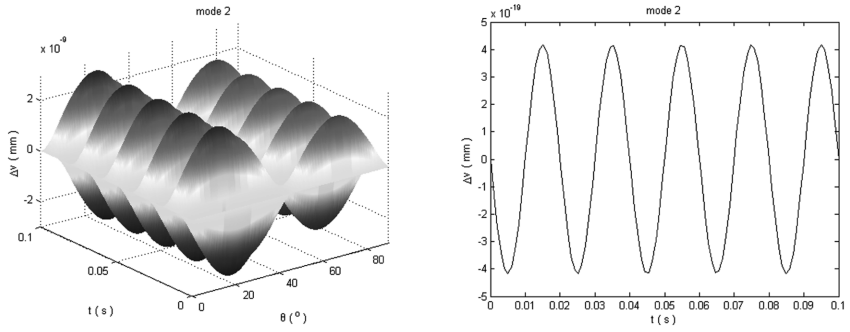

(d) Tangent forced response displacement (mode two)

Fig. 4 Forced response displacements (modes 1 and 2)

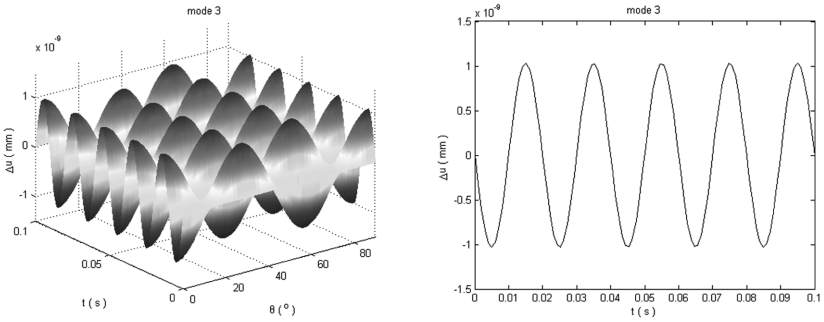

(a) Radial forced response displacement (mode three)

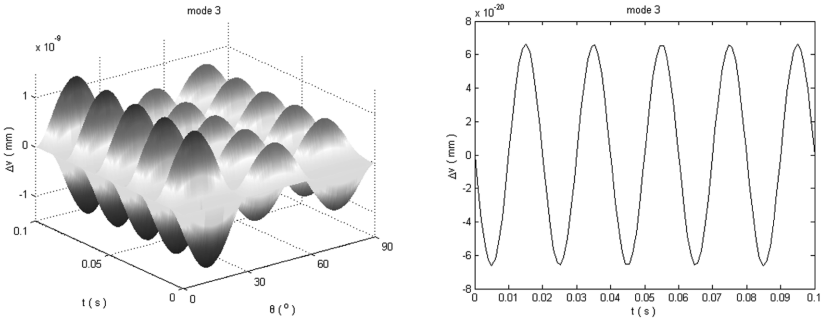

(b) Tangent forced response displacement (mode three)

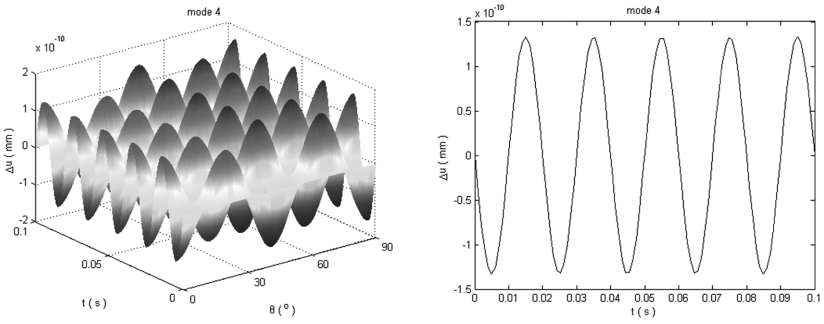

(c) Radial forced response displacement (mode four)

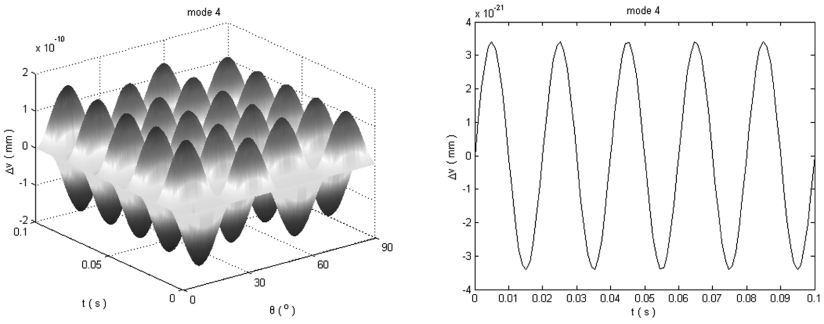

(d) Tangent forced response displacement (mode four)

Fig. 5 Forced response displacements (modes 3 and 4)

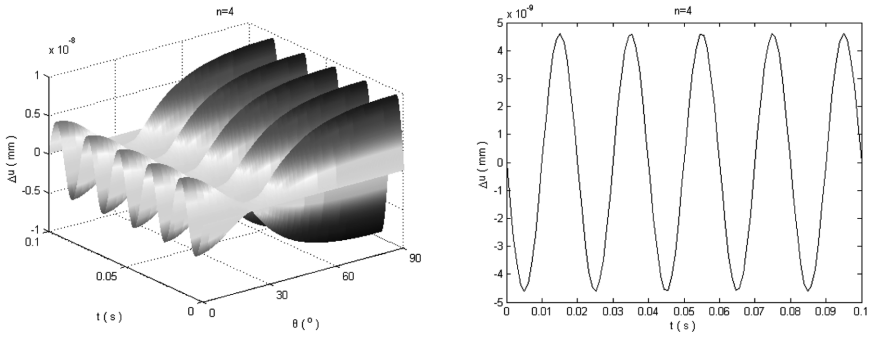

(a) Total radial forced response displacement (n = 4)

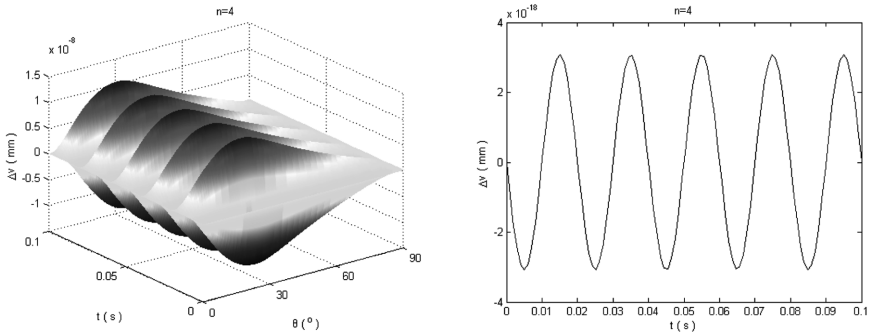

(b) Total tangent forced response displacement (n = 4)

Fig. 6 Total forced response displacements

forced responses are given as shown in Figs. 4-6. Here, only the first four modes are considered, the static voltage v_{si0} = 60*V*, exciting voltage v_a = 10*V*, and exciting frequency ω_z = 314 rad/s. The right figures of the Figs. 4-6 shows forced responses at one point (θ = 0°) on the micro flexible ring. From Figs. 4-6, following observations are worth noting:

(1) For different modes, the voltage excitation can cause the radial and tangent forced responses of the flexible ring.

(2) For given simple harmonic voltage excitation, the forced responses are also simple harmonic vibration. The frequency of the forced responses equals exiting one.

(3) As the exciting voltage frequency is very low compared with the natural frequency of the flexible ring, the forced response magnitude corresponding to mode 1 is the largest, and the total forced response is near one of the mode 1.

(4) The radial forced responses of the ring are much larger than those of the tangent forced responses at point θ = 0°. At other points, the radial forced responses of the ring are near ones of its tangent responses.

(5) As the order number of the vibrating mode increases, positions of the peak dynamic displacements increase and the periodic times and magnitudes of the mode functions decrease.

(6) For different order number of the vibrating modes, the peak displacements of the radial forced responses are as the same order of the amplitude as that of the tangent responses. Hence, when the tangent responses are investigated, the radial forced responses should be considered as well. The radial vibration of the flexible ring can cause unfavorable dynamic behavior such as

speed fluctuation, etc.

The forced frequent responses and their changes along with system parameters are shown in Fig. 7. Here, only results at the point $\theta = \pi/4$ of the first mode are given. From Fig. 7, it is known:

(1) As the exciting frequency is near natural frequency of the system, the radial and tangent

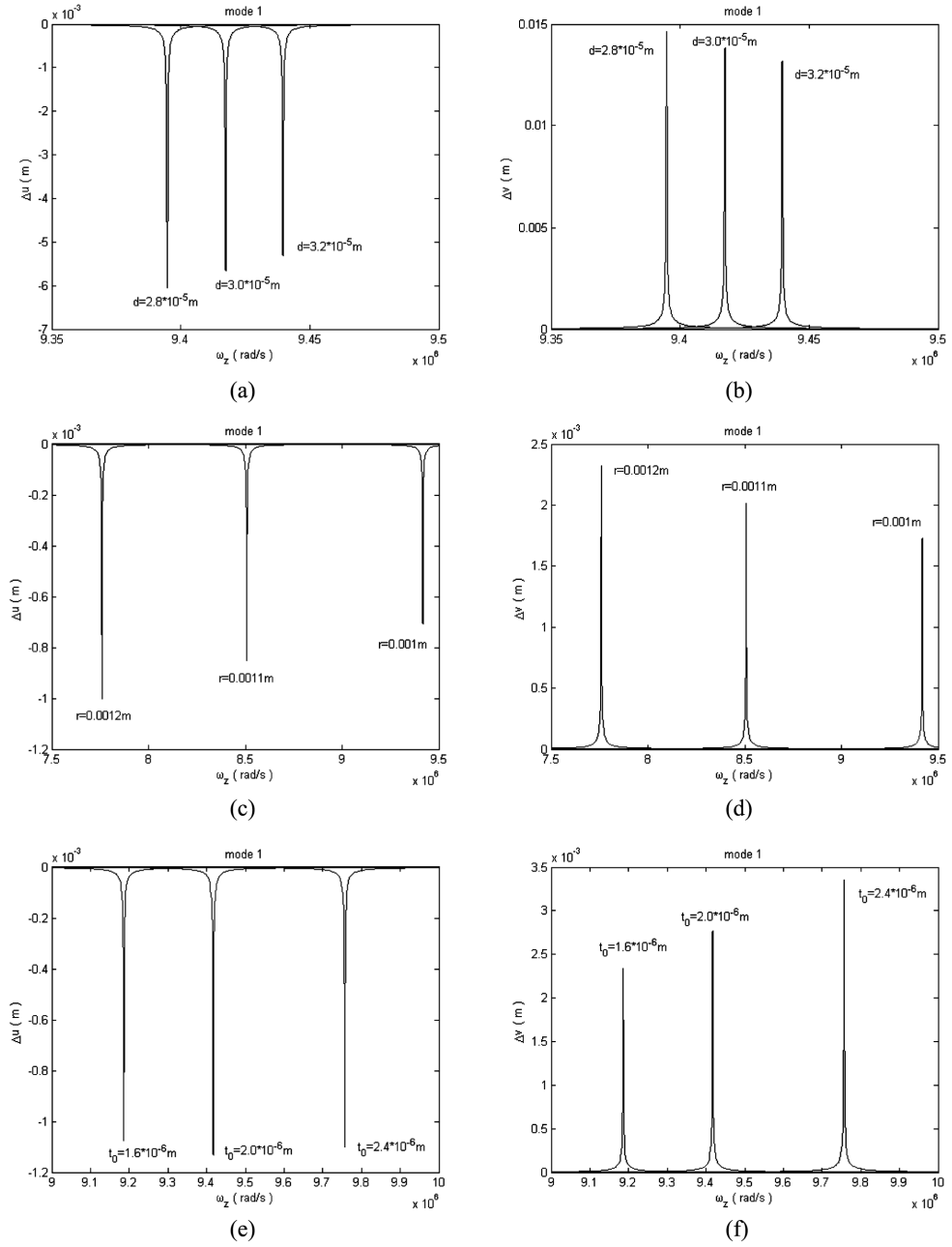

Fig. 7 Changes of the forced response along with the main parameters; (a) change of Δu along with d, (b) change of Δv along with d, (c) change of Δu along with r, (d) change of Δv along with r, (e) change of Δu along with t, (f) change of Δv along with t

resonances all occur.

(2) As the thickness d of micro ring increases, the natural frequencies increase and the radial and tangent vibrating magnitudes of the ring decrease. It is because the system stiffness increases with increasing thickness d.

(3) As the ring radius increases, the natural frequency decreases and the radial and tangent vibrating magnitude of the ring all increase. It is because the system stiffness decreases with increasing ring radius.

(4) As the clearance t increases, the natural frequency increases and the radial vibrating magnitude of the ring do not nearly change, but tangent vibrating magnitude of the ring increase obviously. It is because the system stiffness and equivalent exciting force all increase with increasing clearance t. For tangent vibration, influence of the equivalent exciting force change is principal. For radial vibration, influence of the equivalent exciting force change is near one of the system stiffness change.

(5) In order to get good dynamic performance, smaller clearance t, thickness d and ring radius should be selected.

5.2 Discussions

(1) As above stated, compared with radius of the ring, the transverse section size of the micro flexible ring is so small and Eq. (21) is obtained. Eq. (21) is mainly for the tangent vibration of the flexible ring. However, the study results show that the radial vibration amplitudes are as the same order of the amplitudes as the tangent vibration. Hence, the radial vibration and its effects should be considered in dynamic design of the drive system.

(2) The radial vibration of the flexible ring causes capacitance fluctuation between the stator and the flexible ring. It causes the output speed fluctuation which is analyzed as below:

There is not mechanical input in the drive system. It is similar to a motor and its input is the voltage. The driving torque is

$$T_e = -\frac{1}{2} v_{is}^2 \frac{dC}{d\theta}$$

Where θ is the position angle of the flexible ring.

As the harmonic drive principle is used in the system, there is obvious difference between the drive and the motor. If the speed ratio of the drive is defined as the ratio of the electrical field rotational speed to the flexible ring rotational speed, a large speed ratio is achieved. Thus, the large output torque can be obtained as well

$$T_{out} = iT_e$$

Where i is the speed ratio of the drive system, $i = -r_s/(r_s - r_f)$, r_s is inside radius of the stator, r_f is outside radius of the flexible ring, minus means that the flexible ring rotates in the opposite direction compared to the electric field rotation.

As the clearance between the flexible ring and the stator can be taken to be quite small, the speed ratio is quite large. For example, the speed ratio is 200 under r_s = 1 mm and $(r_s - r_f)$ = 5 μm.

From above equations, it is known that the capacitance change will cause the torque change which can result in the speed fluctuation. In order to remove the speed fluctuation, a compensation

control voltage should be used. Hence, the research results can be used to design the control system of the drive.

(3) As above stated, the flexible ring radius, ring thickness and clearance between the ring and stator have obvious influences on the double displacement coupled forced responses. In order to get good dynamic performance, smaller clearance, thickness and ring radius should be selected.

After the drive parameters are determined, the natural frequencies of the drive system are determined. For avoiding resonance, the exciting frequency should be taken to be far from the natural frequences. Hence, the study results can be used to design operating parameters of the drive system.

(4) When the voltage is stable, considering high order term and Eq. (18) is changed into

$$\Delta F_e = -\frac{1}{2}v_{is0}^2\left.\frac{d^2C}{dw^2}\right|_{w_0}\Delta w\left\{1+\frac{1}{2}\frac{\left.\frac{d^3C}{dw^3}\right|_{w_0}}{\left.\frac{d^2C}{dw^2}\right|_{w_0}}\Delta w\right\} = -\frac{1}{2}v_{is0}^2\left.\frac{d^2C}{dw^2}\right|_{w_0}\Delta w\left\{1+\frac{3}{2}\frac{\Delta w}{t-\bar{u}_0+d_c/\varepsilon_r}\right\}$$

Simulation results shows: $\frac{3}{2}\frac{\Delta w}{t-\bar{u}_0+d_c/\varepsilon_r} \le 0.019$ (here $\Delta w/t \le 0.5\%$).

Thus, the error neglecting the high order term is 1.9%. Hence, nonlinear elastic effects can be neglected. If $\frac{3}{2}\frac{\Delta w}{t-\bar{u}_0+d_c/\varepsilon_r} = 0.1$ (here $\Delta w/t = 3\%$), the error neglecting the high order term is 10%. Therefore, when the amplitude of dynamic displacement gets to 3% of the clearance between the stator and the flexible ring, nonlinear elastic effects should be considered. For example drive system, if the amplitude of the exciting voltage is increased by 6 times, nonlinear elastic effects should be considered. Otherwise, as the exciting frequency of the exciting voltage is near to the natural frequency of the drive system, nonlinear elastic effects should be considered as well.

(5) When the flexible ring vibrates, the damping comes mainly from the film air pressure between the stator and the flexible ring. When the vibrating frequency of the ring is not very high, the air damping is quite small and can be neglected. For simplifying analysis, the damping is neglected in the paper. The research results are useful for designing the dynamic performance of the drive system under condition that the exciting frequency is not very high. Of course, it is also useful for high frequency vibration analysis of the drive system under vacuum. Meanwhile, the results can be taken as basis for high frequency vibration analysis where the air damping should be considered.

6. Conclusions

In this paper, the double displacement coupled statics and dynamics of the electromechanical integrated electrostatic harmonic drive are developed. The linearization of the nonlinear dynamic equations is completed. The double displacement coupled forced response of the drive system to voltage excitation are obtained. Changes of the forced response along with the system parameters are given. The results can be used to design and manufacture of the drive system and can offer some reference for other micro electromechanical systems.

Acknowledgement

This project is supported by the National Natural Science Foundation of China (No50775195).

References

Bao, Z.P. and Mukherjee, S. (2004), "Electrostatic BEM for MEMS with thin conducting plates and shells", *Eng. Anal. Bound. Elem.*, **28**, 1427-1435.

Giuseppe, M. (2007), "Design and demonstrators testing of adaptive airfoils and hingeless wings actuated by shape memory alloy wires", *Smart Struct. Syst.*, **3**(1), 89-114.

Lizhong, Xu. and Xiuhong, Hao. (2007), "Dynamic response for electromechanical integrated toroidal drive to electric excitation", *Struct. Eng. Mech.*, **26**(6), 635-650.

Nadal-Guardia, R., Brosa, A.M. and Dehe, A. (2003), "AC transfer function of electrostatic capacitive sensors based on the 1-D equivalent model: application to silicon microphones", *J. Microelectromech. S.*, **12**(6), 972-978.

Oliver, B. (2000), "Harmonic piezodrive-miniaturized servo motor", *Mechatronics*, **10**, 545-554.

Sarros, T., Chew, E.C., Crase, T.S., Tay, B.K. and Soong, W.L. (2002), "Investigation of cylindrical and conical electrostatic wobble micromotors", *Microelectronics*, **33**, 129-140.

Thielicke, E. and Obermeier, E. (2000), "Microactuators and their technologies", *Mechatronics*, **10**, 431-455.

Wu, X.S., Chen, W.Y. and Zhao, X.L. (2006), "Development of a micromachined rotating gyroscope with electromagnetically levitated rotor", *J. Micromech. Microeng.*, **16**(10), 1993-1999.

Xu, L., Qin, L. and Zhu, C. (2007), "Electromechanical integrated electrostatic harmonic actuator", *Proceedings of the Institution of Mechanical Engineers, Part I: Journal of Systems and Control Engineering*, **221**(3), 487-495.